An extended period of extremely weak geomagnetic field suggested by palaeointensities from the Ediacaran Grenville dykes (SE Canada).

Daniele Thallner[1*], Andrew J. Biggin[1], Henry C. Halls[2]

[1]Dept. of Earth, Ocean and Ecological Sciences, University of Liverpool, L69 3BX, UK

[2]Department of Earth Sciences, University of Toronto, 22 Russel Street, Toronto, Canada M5S 3B1

[*]Corresponding author:
Daniele Thallner
Email: daniele.thallner@liverpool.ac.uk
Address: Dept. Earth, Ocean and Ecological Sciences, University of Liverpool, L69 3BX, UK

Keywords: Paleointensity; Ediacaran; Laurentia; Grenville Dykes

Abstract

Long-term variations of the geomagnetic field, observed in the palaeomagnetic record, have the potential to shed much light on the evolution of Earth's deep interior. With a geomagnetic field characterised by anomalous directions and ultra-low intensities, the Ediacaran period (635-538 Ma) is a time of special interest. Steep and shallow directions, leading to virtual geomagnetic poles (VGPs) separated by angles of up to 90° and very close in age could have recorded a geomagnetic field switching between axial and equatorial dipole-dominated states. Alternatively, the field may simply have been highly nondipolar and subject to rapid reversals. Palaeointensity determinations of units that record the anomalous directions could potentially help to discriminate between morphologies but the spatial and temporal distribution of palaeomagnetic data require improvement. Here we present new palaeointensities from 6 dykes from the western end of the Grenville Dyke swarm that recorded directionally anomalous geomagnetic fields around ~585 Ma. Results from double-heating Thellier experiments failed to satisfy the used selection criteria, but successful microwave Thellier, Shaw and pseudo-Thellier experiments lead to palaeointensities that show field strength values of 2.9±2.2 μT and corresponding virtual dipole moments of 0.3-1.7 x10^{22} Am^2. These field strengths are an order of magnitude weaker than the present-day field. VGPs grouping in two distinct clusters with almost identical angular dispersions of VGPs (S_B = 18.5° and 18.9°) may argue for the presence of an equatorial dipole. In contrast, the palaeointensities associated with the steep and shallow components are indistinguishable. Although based on a low number of results, this observation, together with the overall very large VGP dispersion may rather support that the Grenville Dykes have recorded enhanced secular variation linked to a highly unstable and rapidly reversing field.

1. Introduction

Extreme climatic changes in the late Neoproterozoic (Evans and Raub, 2011) and tectonic activity between the final breakup of Rodinia and the assembly of Gondwana have made the Ediacaran period (635-538 Ma, Xiao and Narbonne, 2020) a prime target for palaeomagnetic and geodynamic research. During this period, the individual drifting histories of Laurentia and Baltica remain mysterious (Li et al., 2013) although both their positions are relatively well constrained around the beginning and the end of the Ediacaran at ~615 Ma and from ~550

Ma (McCausland et al., 2014; Meert, 2014). Anomalous directional data in palaeomagnetic datasets leading to ambiguous apparent polar wander paths (APWP) throughout the Ediacaran and parts of the Cambrian have puzzled palaeomagnetists for decades. These APWPs were based on almost orthogonal steep and shallow primary directional components that are extremely close in age and would require unprecedented continental plate velocities to occur in the framework of a geocentric axial dipole field. First attempts to explain this issue led to the proposition of inertial interchange true polar wander (IITPW) events (Kirschvink et al., 1997) – a hypothesis that was met with resistance in parts of the palaeomagnetic community (Torsvik, 1998) and was later labelled as geodynamically implausible (Tsai and Stevenson, 2007). Subsequent studies of APWPs for Laurentia (Hodych et al., 2004) and Australia (Schmidt and Williams, 2010) did not confirm the proposed IITPW and more attention was given to the possibility of an anomalous behaviour of the geomagnetic field itself. In this case, the steep and shallow directions have been interpreted as being caused by the geomagnetic field flipping between an axial and an equatorial dipole field configuration (Abrajevitch and Van der Voo, 2010) or as showing an intermediary state of an axial dipole field during continuous reversals (Halls et al., 2015). Numerical geodynamo simulations have suggested that the occurrence of a protracted equatorial dipole field may be possible during the reversal of an axial dipole field (Aubert and Wicht, 2004; Gissinger et al., 2012) with significant differences between the intensities of the axial and equatorial field states. Questioning the primary nature of anomalous directions, new studies revisited sites that recorded these directions. Analysis of single domain particles in single silicate crystals of the Sept Îles Complex showed that only the shallow components were recorded in single domain carriers and did not confirm the primary nature of the steep component, eliminating the need of IITPW to explain these directions (Bono and Tarduno, 2015). In contrast, new palaeomagnetic analysis of the Grenville Dykes confirmed the existence of several directional components (Halls et al., 2015). The two polarities recorded in the Sept Îles complex and the complex magnetisations of the Grenville Dykes pointed to an unstable and rapidly reversing field as explanation for the anomalous data (Bono and Tarduno, 2015; Halls et al., 2015). The overall paucity of spatial and temporal coverage of palaeomagnetic data in the Ediacaran still impedes a definitive characterisation of the geomagnetic field (Meert, 2014) and new contributions of complex palaeomagnetic signals, that prefer interpretations with the IITPW hypothesis (Robert et al., 2017), may also be compatible with a more complex field geometry during a period of rapid reversals. Studies of magnetostratigraphic data from the late Ediacaran and the early Cambrian (Bazhenov et al., 2016; Levashova et al., 2021), resulting in reversal frequencies of more than 20 reversals/Myr, claim that the field might have been in a hyperactive state at that time. Due to the correlation between reversal frequency and dipole field strength (Kulakov et al., 2019; Tarduno and Cottrell, 2005; Tauxe et al., 2013) the dipole field strength in the Ediacaran is expected to be low. First palaeointensity studies of Ediacaran rocks from Canada (Bono et al., 2019) and Ukraine (Shcherbakova et al., 2020) show ultra-low virtual dipole moments (VDM) that are an order of magnitude weaker than dipole moments in the Phanerozoic. To date, similarly low dipole moments have only been found in the Devonian (Hawkins et al., 2019; Shcherbakova et al., 2017) and the Jurassic (Kulakov et al., 2019; Tauxe et al., 2013). Information about reversals and palaeointensities are critical to delineate the anomalous field behaviour in the Ediacaran. However, no estimates for the strength of the geomagnetic field exist for the early-mid Ediacaran before 580 Ma. Here we report multi-method palaeointensity measurements performed on mid-Ediacaran age units showing both steep and shallow directions to look for differences that could help explain the directional observations of that time.

2. Materials and methods

2.1. **Sample material:**

The samples from dykes within the Grenville province used in this study were collected in Halls et al. (2015) and were taken preferentially from chilled margins. Several dykes were sampled at multiple sites over distances of up to 150km across and along the dyke strike. Analysis of geochemical composition helped with longitudinal correlation of the dykes. Samples were selected for intensity determination if sister-samples from the same site showed a stable component of characteristic remanent magnetisation (ChRM) in the previous study, which was the case for 99 samples from 15 sites within nine dykes (Figure 1). Following the naming convention used in Halls et al. (2015), the five dykes analysed in this study were: Coniston dyke (sites GD02, GD33), French River dyke (GD23), Key River dyke (GD10, GD15, GD16, GD19, GD37) and Sand Bay dyke (GD29). Additionally, four sites from other dykes in the area associated with the dyke swarm (GD07, GD25, GD26, GD30) were also analysed. U-Pb ages exist for Sand Bay dyke (585.2±0.8 Ma), Augusta Lake dyke (584.8±0.6 Ma), Key River dyke (587.3±0.7 Ma) and French River dyke (598.0±1.4 Ma) (Halls et al., 2015).

Differences in chemical composition between the individual dykes suggest single intrusion events at different development stages of the magma chamber (Halls et al., 2015). The directional results in Halls et al. (2015) show four components resulting in antipodal steep and shallow directions close to directions of older studies of the Grenville dykes (e.g. Hyodo and Dunlop, 1993). Positive contact (Halls et al., 2015) and reversal tests (Hyodo and Dunlop, 1993) support the primary nature of the steep direction. This comprises the steep up component B (D:131.2°,I:-70.9°,α_{95}:11.3°) that can be seen in sites of the Key River dyke (Halls et al., 2015) and the approximately antipolar component E, seen in one site of the French River dyke (D:294°,I:74.1°,α_{95}:5.1°), and indistinguishable from the primary direction of the 585.9Ma Mattawa dyke (D:298°,I:72°,α_{95}:7°, Hyodo and Dunlop, 1993). The shallow component from the almost antipolar components C and D can also be observed continuously in sites of the same dyke and component D differs significantly from the regional overprint recorded in the close-by Whitestone anorthosite (Ueno et al., 1975). Because of an inconclusive contact test, it cannot be excluded that the shallow component was remagnetised (Halls et al., 2015). In this study, we nevertheless analysed samples from sites that recorded both steep and shallow components.

2.2 Methods:

All measurements were carried out at University of Liverpool's Geomagnetism Laboratory. To assess the rocks' suitability for palaeointensity determination, at least two specimens per site were selected for rock magnetic measurements. Measurements of isothermal remanent magnetisation, hysteresis loop parameters and thermomagnetic curves were done on a Variable Field Translation Balance using both crushed specimens and cylinder specimens with a diameter of 5mm. Hysteresis loop parameters were processed and analysed in HystLab (Paterson et al., 2018). Temperature dependent susceptibilities were measured on an AGICO MFK-1A Kappabridge using crushed specimens heated in air to 700°C. To monitor thermochemical alterations in more detail, the same measurements were also performed in incremental heating and cooling cycles in temperature steps of 100°C between 150°C and 650°C. Scanning electron microscope (SEM) images were taken with a Hitachi TM3000 tabletop microscope and analysed with Quantax70.

The magnetic viscosity of 59 specimens was determined by measuring their remanent magnetisation after being stored for three weeks in different orientations without shielding from the ambient field (Prévot, 1981). For this experiment, the specimens were stored on a rack in the laboratory with their z axis parallel to the field lines of the geomagnetic field for the first duration and antiparallel to the field lines for the second duration. The remanent magnetisations were measured on an AGICO-JR6 spinner magnetometer.

A multi-method approach was used to measure palaeointensities in an effort to strengthen the quality of our determinations by demonstrating consistent results obtained from fundamentally different methods (DeGroot et al., 2013). Here we used thermal and microwave-Thellier, pseudo-Thellier and double-heating Shaw methods. Microwave-Thellier palaeointensity experiments were performed on the high frequency (14GHz) microwave system and SQUID magnetometer (Suttie et al., 2010). This instrument uses unoriented cylinder specimens with a 5mm diameter. These were drilled from the available 1" cylinders, which allowed for 5 to 15 sub-specimens to be drilled from one standard cylinder specimen. This allowed for a large number of fast palaeointensity experiments (~90 minutes/specimen) to be done despite the low amount of available sample material. Specimens are subjected to microwave treatment with incrementally increasing power and/or duration in a range between 20W·s and 500W·s. The succession of zero-field and in-field steps for the experiments followed the IZZI protocol (Tauxe and Staudigel, 2004). Checks of reproducibility of partial thermoremanent magnetisations (pTRM) were done after every other I-Z-pair, resulting in 4-5 pTRM-checks per specimen. To detect multidomain effects, the laboratory field was applied in angles of 45°-90° to the ChRM of the specimen (Yu and Tauxe, 2005). The laboratory field itself was varied between 3 and 30µT between experiments to detect possible field dependencies of the results.

Thermal-Thellier experiments were undertaken using the IZZI-protocol with pTRM checks in vacuum, using an MMTD80 oven with a bias field of 10µT in the temperature range of 100°C-550°C. Magnetisations of the specimens were measured on an AGICO-JR6 spinner magnetometer after applying a 2mT alternating field (AF) demagnetisation step before every measurement using an AGICO-LDA5 AF demagnetiser to ensure no spurious magnetisations affected the specimen.

In addition to the microwave and thermal-Thellier experiments, that are both based on the same method and therefore potentially prone to being biased by non-ideal carrier effects in similar fashions (e.g. sagging of Arai plots due to MD grains (Smirnov et al., 2017)), the double-heating Shaw method (Tsunakawa and Shaw, 1994) used AF demagnetisations and acquisitions of anhysteretic remanent magnetisations (ARM). These experiments were carried out on a 2G-RAPID superconducting rock magnetometer system in incremental steps of 2-10mT up to a peak AF-field of 100mT. ARMs were given at peak AF-field in bias fields of 57.9µT or 81.2µT. The specimens were given a full TRM twice by heating them to 610° or 650°C in bias fields of 5µT or 10µT to be able to apply an ARM correction (Rolph and Shaw, 1985).

The pseudo-Thellier method (de Groot et al., 2013; Paterson et al., 2016) was performed on the automatic 2G-RAPID system with the same AF levels as used in the Shaw method. This was done to have results that avoided heating the specimen at all during palaeointensity determination. Absolute intensity values were calculated using the generalised calibration from Paterson et al. (2016). Since different pseudo-Thellier calibrations are disagreeing in the expected weak field range (Paterson et al,. 2016; DeGroot et al., 2013), the pseudo-Thellier results were only used for comparison with the measurements made using other methods.

For the purpose of this experiment, bias fields of 11.4μT and 81.2μT were used for the ARM acquisition and, in some cases, Shaw and pseudo-Thellier experiments were run as a combined experiment, where the ARM acquisition steps were performed instead of the single ARM magnetisation at peak AF field in standard Shaw experiments.

For thermal and microwave-Thellier experiments, the selection criteria followed the Standard Palaeointensity Definition (SPD, Paterson et al., 2014) and were modified from the SELCRIT2-criteria (Biggin et al., 2007a). The criteria of N=4, FRAC≥0.35, ß≤0.1, q≥1, MAD≤15°, α≤15°, DRAT≤10% and CDRAT≤10% were used together with a curvature factor if the best-fit line (Paterson, 2011) of |k'|≤0.27.

The selection criteria used for the Shaw method were similar to those set out by Yamamoto et al., (2010),: number of consecutive data points N≥5, correlation coefficients of the linear parts of the NRM-TRM1* diagram and the TRM1-TRM2* diagram of $r^2_N \geq 0.995$ and $r^2_T \geq 0.995$, the fraction of used NRM f≥0.2 and the slope of the linear part of the TRM1-TRM2* diagram $0.95 \leq slope_T \leq 1.05$. In addition, the selected part of the NRM must appear linear and convergent on the orthographic plot of the NRM demagnetisation with |k'|≤0.27 and with α and MAD values ≤10°.

The SPD selection criteria used for pseudo-Thellier experiments were slightly relaxed from Paterson et al., (2016) and applied to a convergent part of NRM in the orthographic plot: N≥6, f≥0.3, ß≤0.1, $r^2 \geq 0.990$, $f_{resid} \leq 0.15$, α≤10°, MAD≤10°, |k'|≤0.27 and $0.85 \leq |b_{AA}| \leq 1.15$.

Results that passed all criteria were classified as 'A'. Because the selection criteria used in this study for the numerical handling of Arai plot data as a qualifier were stricter than the ones used in other intensity studies of similarly aged rocks (Bono et al., 2019; Shcherbakova et al., 2020), we introduced relaxed values in certain specific cases based on the criteria used by

Shcherbakova et al. (2020). Results that used relaxed criteria were classified as ‘B’. Limits for relaxed selection criteria were: FRAC≥0.25, DRAT≤15%, CDRAT≤15% and |k’|≤0.48 for microwave and thermal Thellier experiments and $r^2_N \geq 0.990$ and $r^2_T \geq 0.990$ for Shaw experiments. Microwave-Thellier, thermal-Thellier and pseudo-Thellier results were analysed with paleointensity.org (Béguin et al., 2020). If multiple fits passed selection criteria, then the fit with the highest number of included points and lowest curvature was chosen.

3 Results

Thermomagnetic curves and susceptibility versus temperature curves measured on samples from different dykes showed quite diverse behaviour (Supplementary Figure 1). Most specimens showed one or two Curie temperatures between 550°C and 580°C. Heating curves for specimens from the French River and Key River dykes as well as specimens from sites GD25 and GD26 also had noticeable Hopkinson-like peaks, often indicating the presence of single-domain (SD) or pseudo-single-domain (PSD) magnetic phases. Apart from small alterations around 400°C, heating and cooling curves of cyclic experiments were reversible up to 550°C. Considerable alterations occurred in the temperature range between 550°C and 650°C and features such as Hopkinson like peaks were not visible in the final cooling curve of the last cycle. Exceptions related to higher levels of weathering were measurements on specimens from site GD01 with a Curie temperature of 470°C and from sites GD07 and GD30, where susceptibilities were about two orders of magnitude weaker. Accordingly, no palaeointensity estimates were obtained from these sites. The susceptibility curves of specimens from Coniston, French River and Sand Bay dykes showed a small ‘toe’ with another Curie temperature up to 610-620°C, possibly suggesting the presence of a small fraction of maghemite or titanohematite. Backscattered electron imaging (Figure 2a-c) shows relatively coarse (~30-200µm) (Ti-)magnetite grains with sharp edges as well as small dendritic (<~40µm) (Ti-)magnetite grains (e.g. Figure 2a,b), indicating rapid cooling of the rocks. Energy dispersive spectroscopy elemental composition mapping of larger grains shows structures of full and partial exsolutions with lamellae of titanium-rich ilmenite and titanium-poor magnetite (Figure 2c, Supplementary Figure 2). The preservation of high-temperature textures and lack of low-temperature oxidation structures suggest that the grains are carriers of a primary TRM. For some samples it cannot be ruled out that the oxy-exsolution continued to temperatures lower than the Curie temperatures. Thermochemical remanences (TCRM) from such processes have been connected to underestimates of Thellier data (Smirnov and Tarduno, 2005). More recently, a study on rocks with artificially induced TCRMs found contrasting results showing only small effects on their resulting palaeointensities (Shcherbakov et al., 2019).

Hysteresis parameters (Figure 2d-f) fall in two clusters on the Day et al., (1977) plot with one large cluster in the "PSD" area and several data points at lower ratios of magnetic remanence to saturation magnetisation (M_{rs}/M_s) and higher ratios of remanent coercivity to coercivity (Bcr/Bc) indicating a mixture of magnetic domain types with both single-domain and multidomain grains. However, all samples show reasonably high bulk domain stability (Paterson et al., 2017) with positive values between 0.08 and 0.63 (Figure 2d) implying that the rocks may give good palaeointensity results. Hysteresis loops of weathered samples (sites GD07, GD30) show large paramagnetic contributions, probably carried by clays. Comparison of hysteresis parameters with the theoretical predictions for titanomagnetites $Fe_{3-x}Ti_xO_4$ with x=0 (TM0) and x=0.6 (TM60) (Wang and Van der Voo, 2004) shows that most specimens plot close to the TM0 line. This includes results from the French River dyke, which showed a substantially higher TiO_2-content in the geochemical analysis of the sites in Halls et al. (2015). In contrast, specimens from the low-Ti-type Coniston dyke (Halls et al., 2015) plot further away from the TM0 and closer to the TM60 line.

Fractions of viscous remanent magnetisations (VRM) of specimens from the different sites, acquired after 3 weeks in the ambient field, did not show any differences at the dyke level. The average viscosity index (*v*) for all sites was 14.4% (median=9.6%, stdev=14.9%). This mean viscosity index includes *v* values of up to 80% from sites GD07 and GD30. Specimens from those sites had very low magnetisations and the viscosity index was mostly calculated from noise. Specimens with *v* values of >30% were not used for intensity determination. We note that low palaeointensities will naturally produce weak NRMs (on account of Thellier's law of linearity (Thellier, 1941)) which will then be more radically affected by a VRM acquired in the strong present-day field.

Microwave demagnetisation experiments were performed on 29 specimens to determine their response to microwave treatments. These measurements showed that it was possible to demagnetise specimens from all sites with microwave treatment. However, specimens from the weathered sites GD07 and GD30 as well as host rock specimens from site GD29 were too weakly magnetised to be measured on the microwave system. In total, palaeointensity measurement was attempted on 204 specimens of the Grenville dykes. Of these, 127 used microwave-IZZI, 20 used thermal-IZZI, and 57 used Shaw and/or pseudo-Thellier experiments (Table 1). A relatively small number of thermal Thellier experiments were attempted because these were inefficient in terms of the amount of material used, the time taken to perform, and the degree of alteration produced by repeated heatings in air. In any case, the microwave

Thellier approach has been shown to give equivalent, or better, results in many studies when the same protocols were followed (Biggin et al., 2007b; Grappone et al., 2019, 2020).

In the relatively small number of thermal Thellier experiments, specimens universally showed non-ideal behaviour and did not pass selection criteria. These mostly produced chaotic Arai and orthographic plots (Figure 3e) and the experiment was stopped at 550°C. Strong 'zig-zagging' and high β values together with high curvature values suggest strong MD behaviour over the full temperature range that was seen in all experiments. In contrast, for about half of the specimens pTRM checks passed the criteria up to the highest temperature steps.

The majority of Arai plots from all Thellier experiments (75%) and of passing Thellier results (94%) showed two slopes. Similar to the results of other studies yielding extremely low palaeointensities (Hawkins et al., 2019; Shcherbakova et al., 2020), the sharp bend between the high- and low-temperature/power slopes usually coincided with the junction between ChRM and secondary components in the associated Zijderveld plots (Figure 3a,c), but this was not clearly visible for all results (Figure 3b, Figure 5a-d). For results that do not show a clear directional change (Figure 3b) it can be difficult to ascertain whether a two-sloped Arai plot is due to large palaeointensity differences between ChRM and overprint or due to a sagging of the slope caused by MD grains. Here, zig-zagging and curvature were used as prime criteria to detect and reject results biased by MD behaviour. Of the accepted microwave Thellier results, 6 passed as A and 19 as B result. For all B results, DRAT, CDRAT or curvature had to be relaxed. About 10% of the results that were not accepted failed only one of the selection criteria. All other rejected results failed more than one selection criterion (e.g. Figure 3e). The most commonly failed criteria were β (57% of results), FRAC (56%), DRAT/CDRAT (48/52%) and k' (30%). The high failure rate due to β, k' and DRAT/CDRAT shows that MD effects and mineral alterations during heatings were both primary issues in the results of thermal and microwave experiments. Six low-temperature/power slopes (5%) would pass the selection criteria, but it is clearly visible in the orthographic plot that the selected fraction is not the ChRM (Figure 3d). One outlier intensity from a high-power slope of 26.7μT passed the selection criteria (GD19-43B1) but was rejected as unreliable because the standard deviation of possible intensities from the high-power slope of sister specimens of this sample was larger than the mean intensity.

Of the 12 accepted Shaw results, 7 passed as A and 5 as B results. For all 7 B results, the correlation coefficient of the best fit line in the NRM-TRM1* plot r^2_N was relaxed to $r^2_N \geq 0.990$ (Figure 4a). Results not passing r^2_N, k' and/or $slope_T$ was the main reason for unsuccessful experiments. Multidomain effects in Shaw experiments can cause biased ARM corrections and often lead to non-linear Shaw plots (Tanaka and Komuro, 2009). Here, rejected results with correlation coefficients of $r^2_n \leq 0.95$ also showed high curvatures while in turn, linearity of Shaw plots was high ($|k'|=0.1\pm0.05$) for results that passed as A or B (Figure 5e). Validity of ARM corrections is checked in the double heating method and four results with linear Shaw plots were rejected because a failed ARM correction was detected in the plot of the TRM of the first heating versus the ARM corrected TRM of the second heating. Specimens showed a wide range of coercivities with an average median destructive field MDF=19.2±9.6mT. Eight specimens were too weakly magnetised to generate ChRMs during demagnetisation. Secondary magnetisations that accounted for NRM fractions of up to 80% were usually removed by AF fields of less than 40mT. Similar to the AF demagnetisation experiments in Halls et al. (2015) that successfully generated reliable directions and passed field tests, the remaining fraction of primary NRM was sufficiently large in the Shaw experiments such that only ~20% of specimens failed the FRAC criterion. The directions gained from analysis of the demagnetisation of NRM were used together with directions from Halls et al. (2015) to recalculate site-mean directions for determinations of VDMs (Table 1).

From the 28 pseudo-Thellier experiments, 5 specimen results passed selection criteria and were accepted. Results from successful pseudo-Thellier experiments, which involve no laboratory heating whatsoever, showed good agreement with the site-mean values calculated from microwave and Shaw results (Table 1). Pseudo-Thellier results from sites GD33, GD29 and GD26 and associated site-means calculated using other methods agree within uncertainty. For sites GD26 and GD37 that show a larger difference (>1μT) between intensities from pseudo-Thellier experiments and intensities from other methods, the palaeointensities from pseudo-Thellier experiments are lower than the palaeointensities from the other methods. Most unsuccessful pseudo-Thellier experiments failed due to a high curvature of the selected line segment in the demag-demag plot (Figure 4b) suggesting that NRM and ARM (de)magnetisations behave differently in these specimens and a palaeointensity calculated from these would be unreliable (Figure 5f).

Combining A and B results, 25 results of the microwave-Thellier experiments (20% success rate) and 12 results of the Shaw experiments (24%) passed the used selection criteria. None of the thermal-Thellier experiments passed selection criteria, leading to an overall success rate of 18% for Shaw and Thellier-type experiments. Palaeointensity estimates were averaged for each dyke as separate spot readings of the field strength (Table 1). The resulting intensity values range from 1.4μT to 7.6μT, and yielded VDMs of 0.3-1.7*10^{22}Am^2. Five pseudo-Thellier results passed selection criteria as well and gave intensity values between 1.1μT and 4.1μT.

All intensity results with critical values are listed in supplementary tables 1-3 and measurement data of all experiments are available on the MagIC database (www2.earthref.org/MagIC).

4 Discussion

The geomagnetic field in the Ediacaran is characterised by ambiguous field directions that impede the construction of reliable APW paths. Recently, it has been stated that the time averaged dipole field strength is uniquely low in the Ediacaran which is seen in both single-crystal (Bono et al., 2019) and whole-rock studies (Shcherbakova et al., 2020). We expand these intensity data with the whole-rock palaeointensities of the Grenville dykes with VDMs of $0.76\pm0.5*10^{22}Am^2$.

Due to the low number of available samples and non-ideal behaviour during thermal-Thellier experiments, microwave experiments were preferred as the small sample size allowed for a high number of experiments with sub-specimens. To account for a possible method-bias of the MW results, a number of thermal-Thellier, Shaw and pseudo-Thellier experiments were conducted as well. All methods suffered from low success rates that made it hard to compare the different methods on the site level. Where such a comparison was possible, the results from different methods differed by less than 1μT, similar to the overall variability on the dyke level. From this, a method related systematic bias seems unlikely. Furthermore, results from Thellier and Shaw experiments are also supported by the results of the pseudo-Thellier experiments. Figure 5 shows a range of rejected and accepted results that show consistent palaeointensities from all methods for sister specimens from a sample of the French River dyke.

To confirm that the intensity results are not biased by the choice of selection criteria, other commonly used sets of selection criteria were used to re-analyse all Thellier-type results (supplementary table 4). All sets show only small differences in the range of ~1µT and agree well with the results of the Shaw experiments. Results from combined A and B results only differ from pure A results by 0.2µT and are well inside the standard deviation of A results, while the number of accepted results almost doubled.

The two-slope behaviour, seen in most Arai plots of Thellier experiments in this study, has been recognised in other studies of basalts with low palaeointensities as well (e.g. Hawkins et al., 2019). Similar behaviour is often ascribed to MD behaviour (Riisager and Riisager, 2001; Smirnov et al., 2017) and/or alteration of magnetic minerals during heating steps of the experiments (Kissel and Laj, 2004) as well as to instabilities of aged thermoremanence (Shaar and Tauxe, 2015). Thermochemical alteration during the heatings was very common in the experiments of this study and results that were affected by alteration, as seen from pTRM checks, were rejected. Curved or zig-zagging Arai plots, caused by MD behaviour and/or instability of TRM, were excluded if the curvature or β criteria were not met. Hawkins et al. (2019) argued that the two-slope behaviour without a corresponding directional change in their study was attributed to strong thermal or thermoviscous overprints of similar direction. This is also the case in our study, but here a directional change is often observable at the bend between the two slopes in the Arai plots as well. Therefore, the slope of the high unblocking temperature ranges, that also carried the ChRM in Halls et al. (2015), were selected in the Arai plots to calculate palaeointensities.

While all steps were taken to detect and reject results biased by MD behaviour, the ambiguity of sagging and two-sloped Arai plots may cause doubt over whether every single biased result was rejected, especially since MD effects were one of the main issues leading to low success rates. The high agreement of results from different methods, however, confers confidence that the accepted mean results were not substantially biased. It is noted that even if palaeointensity errors due to non-ideal carriers were as large as 25% (Smirnov et al., 2017; Tanaka and Komuro, 2009), these would produce a very small absolute bias in the results of this study.

The overall quality of accepted palaeointensity results was assessed by the application of Q_{PI} criteria (Biggin and Paterson, 2014) for each dyke (supplementary table 5).

The AGE criterion was met by all dykes as the dyke swarm was radiometrically dated in Halls et al. (2015). Augusta Lake dyke, Key River dyke and Sand Bay dyke met the STAT criterion. The French River dyke has more than the required 5 individual intensity estimates, but the estimate had a dispersion (stdev/mean) ≤25% (Paterson et al., 2010), which is often the case for ultra-low palaeointensity results (e.g. Shcherbakova et al., 2020). Other units yielded less than the 5 successful individual palaeointensity results needed to meet the STAT criterion.

Mostly fresh looking titanomagnetite grains with high-temperature oxy-exsolution structures and rapidly cooled dendritic magnetite grains without signs of low-temperature oxidations as seen from SEM suggest that the magnetisation is a primary TRM. However, concerns can be raised about the validity of the magnetisation itself due to the anomalous nature of the palaeodirections (Halls et al., 2015). This is especially the case for sites associated with the shallow directional component, where the possibility of a remagnetisation event cannot be completely dismissed due to inconsistent results of a baked contact test (Robert et al., 2017). Our rock magnetic data imply a similar range of magnetic mineralogy for samples from sites of either directional component and no systematic differences could be seen that would support a remagnetisation of the shallow component. Halls et al. (2015) argued that these shallow directions are also primary because they are almost antipodal and can be followed continuously along the dyke. Palaeointensity estimates, irrespective of the associated directions were similar and extremely low and the angular dispersions of VGPs show almost identical behaviour of steep and shallow components. On the basis of the combined microscopic and palaeomagnetic evidence for samples of both directional components, we chose to award the TRM criterion to all units.

The use of pTRM checks and the application of the IZZI protocol with β and k' criteria as well as the double heating checks of the Shaw experiments enabled the exclusion of all estimates that could be significantly biased by thermochemical alteration or MD behaviour during the experiments. Therefore, all sites passed both the ALT and MD criteria. Following the standard palaeointensity definitions (SPDv1.1, Paterson et al., 2014), the angle between the laboratory field and the last pTRM check of the Thellier experiments was calculated as $\gamma=3.2°\pm1.2°$, showing that the results were not majorly influenced by anisotropy effects. Systematic bias of estimates due to non-linear TRM behaviour was avoided by using different laboratory TRM fields between 3μT and 30μT and ARM fields between 10μT and 81.2μT. The similarity of results between the Shaw method with cooling times of ~1h and the microwave Thellier method with cooling times of <1min exclude a cooling rate bias. Therefore, the ACN criterion was given to all units.

Four different methods were used to determine palaeointensities. To pass the TECH criterion, the palaeointensity estimate of a unit has to comprise results from at least two different methods which was the case for 5 units. The rejection of all thermal-Thellier results remains troubling as systematic differences between results from thermal and microwave experiments were found in previous studies (Biggin, 2010). Instead of the different demagnetisation methods causing the discrepancies, the bulk of differences has recently been attributed to the failure to detect non-ideal behaviour (Grappone et al., 2020). Grappone et al. (2020) suggested that the use of appropriate protocols in both methods could reduce the differences in results. This is supported by the results of (Shcherbakova et al., 2020) where thermal and microwave experiments using IZZI and Coe protocols produced agreement in Ediacaran-aged rocks. Good agreement of results between the microwave and Shaw/pseudo-Thellier methods in this study gave additional confidence in the reliability of the accepted intensity determinations. The criterion LITH was only awarded to Key river dyke since site GD37 combines results from both the dyke and baked host rocks. All measurement data are available on the MagIC database, awarding the MAG criterion to all units.

Summing up the QPI criteria results in scores of 6-9 indicating that the accepted palaeointensity estimates, despite being low in number and lacking accepted thermal Thellier results, are of high technical quality. A higher number of accepted results would allow the palaeointensities associated with the steep B and shallow C+D directions found in Halls et al. (2015) to be compared. Assuming a high-latitude of Laurentia around ~590 Ma, the palaeointensities of the shallow component – if recording an equatorial dipole field state – might be expected to be much lower than the intensities of the steep component. The number of accepted intensities is insufficient for significant comparison of the two components, but the average site-mean palaeointensities of all sites with shallow directions (3.7±2.3μT) and sites with steep directions (5.0±0.5μT) are within error at one standard deviation. This similarity of the ultra-low palaeointensities of the two components may be a hint that the Grenville Dykes have recorded a highly unstable field as proposed in Halls et al. (2015). In contrast, the high and almost identical values for angular dispersions (supplementary figure 3) of two distinct groups of VGPs around the mean VGPs of the steep (S_B=18.5°) and the shallow component (S_B=18.9°) look consistent with the existence of an equatorial dipole. However, some caution is advised when taking the dispersions at face value. Recent studies of VGP scatter required a minimum of N=9 sites (Doubrovine et al., 2019). After the exclusion of lower quality directions from sites with n≤4 or k≤30 in the calculations, this requirement was only met by the shallow component (N=11), but not by the steep (N=7). The dispersion values seem reasonable for the time period with comparable values for Laurentia showing a wide range between S_B=13.5° (McCausland and Hodych, 1998; Veikkolainen and Pesonen, 2014) and S=~26° (Bono et al., 2019). If the two groups of VGPs were interpreted as one group, showing a transitional field, then the resulting VGP dispersion would be S_B=~33° at low latitude. This would be an extremely high value but the current lack of constraints on the Ediacaran field means that it is not implausible.

With the exception of sites GD14 where only one single intensity was accepted and GD25, where a single high (7.6 and 12.6μT) microwave result leads to high VDMs of ~1.7*10^{22}Am^2, the mean VDMs of 0.6±0.2*10^{22}Am^2 are comparable to the single-crystal results of the Sept Îles (~0.7*10^{22}Am^2,Bono et al., 2019) and the whole-rock results of the Volyn Traps (0.9±0.2*10^{22}Am^2,Shcherbakova et al., 2020). The palaeointensities, coming from dykes with ages that span ~15 million years, could suggest that a sustained geomagnetic field with these extremely low intensities extended back at least until 600 Ma with intensities being an order of magnitude weaker than the strength of the present-day field (Figure 6). Palaeointensities this low have been reported for Earth before, but were generally not attributed to a sustained field. The PINT database (Biggin et al., 2015) contains 6 site-mean estimates with H_{pal}≤5μT or VDM≤0.5*10^{22}Am^2, N>1 and reliable experiment types (excluding single-heating Shaw and total TRM experiments) that can be roughly divided into two groups. The first group comprises entries with mid-Miocene or younger ages that show the ultra-low intensity values in single basalt flows from Iceland (Lawley, 1970) and the Canary Islands (Brown et al., 2009; Leonhardt and Soffel, 2002) that are all connected to the short-term drop of dipole moments during polarity transitions interrupting a much stronger sustained field. The palaeointensities with Mesoproterozoic to Archaean ages from the second group are either (a) extremely low due to fractions of chemical remanent magnetisation (Yoshihara and Hamano, 2004), (b) would not satisfy any modern sets of selection criteria (Ueno, 1995), or (c) are only seen as spot reading of the field in a single dyke showing an anomalously low intensity (Smirnov and Tarduno, 2005) in a population of dykes with higher palaeointensities (Halls et al., 2004). Non-Ediacaran weak sustained fields as in the Jurassic (~2.8 ±0.9*$10^{22}$$Am^2$, Tauxe et al., 2013) or the Devonian (~1.1±0.5*$10^{22}$$Am^2$, Hawkins et al., 2019) are all stronger. However, a field strength behaviour, similar to the one in the Ediacaran, can be observed in the Upper Devonian around ~370 Ma, where site-mean palaeointensities as low as 2.4μT (0.4*$10^{22}$$Am^2$) have been reported in a weak time-averaged field as well (Hawkins et al., 2019).

The similarity of the weak palaeointensities in this study with those seen during reversals and excursions further strengthens the hypothesis of an unstable/transitional and possibly hyperactive field throughout the Ediacaran. Similar to the palaeointensities for the later Ediacaran (Shcherbakova et al., 2020) we cannot exclude that all of our spot readings of the field sample reversals or excursions in a hyper-reversing Ediacaran field and miss periods of stronger fields. Consistency of directional results do not necessarily contradict the intensities belonging to a reversal (e.g. Prevot et al., 1985). However, to date there have been no reports of any stronger fields throughout the Ediacaran and the ultra-low intensities seen in the spot readings of this study and Shcherbakova et al. (2020) agree with estimates of time-averaged intensities in Bono et al. (2019) (Figure 6). To confirm that a sustained weak field does indeed extend back to the mid-Ediacaran – or further – a better data coverage and time-averaged palaeointensities will be required.

These ultra-low Ediacaran intensities are consistent with the predicted weak-field state of the geodynamo before the onset of inner core growth (Bono et al., 2019; Driscoll and Evans, 2016). Under this scenario, the dynamo was operating marginally, powered by thermal convection due to heat loss at the core-mantle-boundary alone and the field was diminished. Subsequently, the inner core nucleated providing additional convective power from the release of light elements and latent heat of crystallisation. We cannot, however, rule out an entirely different cause of a massively diminished dipole moment in the Ediacaran, perhaps related to a reconfigured convective pattern in the core perhaps related to an unusual core-mantle heat flow pattern. That the measured palaeointensities are similar in magnitude to ground measurements of a local crustal field of Mars (Johnson et al., 2020), a planet which is suspected to have been without a core dynamo for 4.1 billion years, raises profound questions concerning measurement limits and the history of the geodynamo.

5 Conclusions

We report new palaeointensities from six dykes at the western end of the Grenville dyke swarm. Success rates of palaeointensity experiments were substantially lowered by the rejection of all samples where thermochemical alteration during laboratory heating or MD behaviour were suspected. Detection of MD behaviour was especially important as non-ideal magnetic carriers were present in the studied rocks and MD behaviour would lead to an underestimate of palaeointensities. The application of strict selection criteria resulted in the rejection of all thermal-Thellier results. The resulting palaeointensity values from Shaw and microwave-Thellier experiments range between 1.4-7.6μT (0.33–1.76*10^{22}Am^2). These estimates agree well with results from other palaeointensity studies from this time period (Figure 6) and suggest that the Ediacaran field might have been weak over a longer time frame than previously seen from palaeointensity data. This opens up questions about what geodynamo regimes could sustain such weak fields over longer time periods. The behaviour of VGPs with almost identical angular dispersion around two clusters argues for the presence of an equatorial dipole field. In contrast, the consistency of presented ultra-low intensities along dykes for both directional components supports the idea of an unstable and/or transitional field in the Ediacaran. The presented data are another argument for the Ediacaran field behaving strangely but at this point, a more precise definition is elusive. Measurements from the early to mid-Ediacaran are still scarce and a better coverage of spot readings of palaeointensity, time averaged palaeointensities and magnetostratigraphic data would be immensely useful to better characterise the geomagnetic field in the Ediacaran.

Acknowledgements

This study was supported by The Leverhulme Trust (Research Leadership Award, RL-2016-080). We would like to thank R.K. Bono, G. Paterson, J. Kavanagh and S. Lloyd for helpful discussions. Henry Halls would like to thank Alan Lovette for helpful field assistance in finding outcrops of dykes that formed negative topographic features and for many of the paleomagnetic measurements. We also thank James Badro and two anonymous reviewers for their helpful comments.

Data availability:

Daniele Thallner, Andy Biggin, Henry Halls (2020) "An extended period of extremely weak geomagnetic field suggested by palaeointensities from the Ediacaran Grenville dykes (SE Canada).", Magnetics Information Consortium (MagIC), 10.7288/V4/MAGIC/16863

Figures:

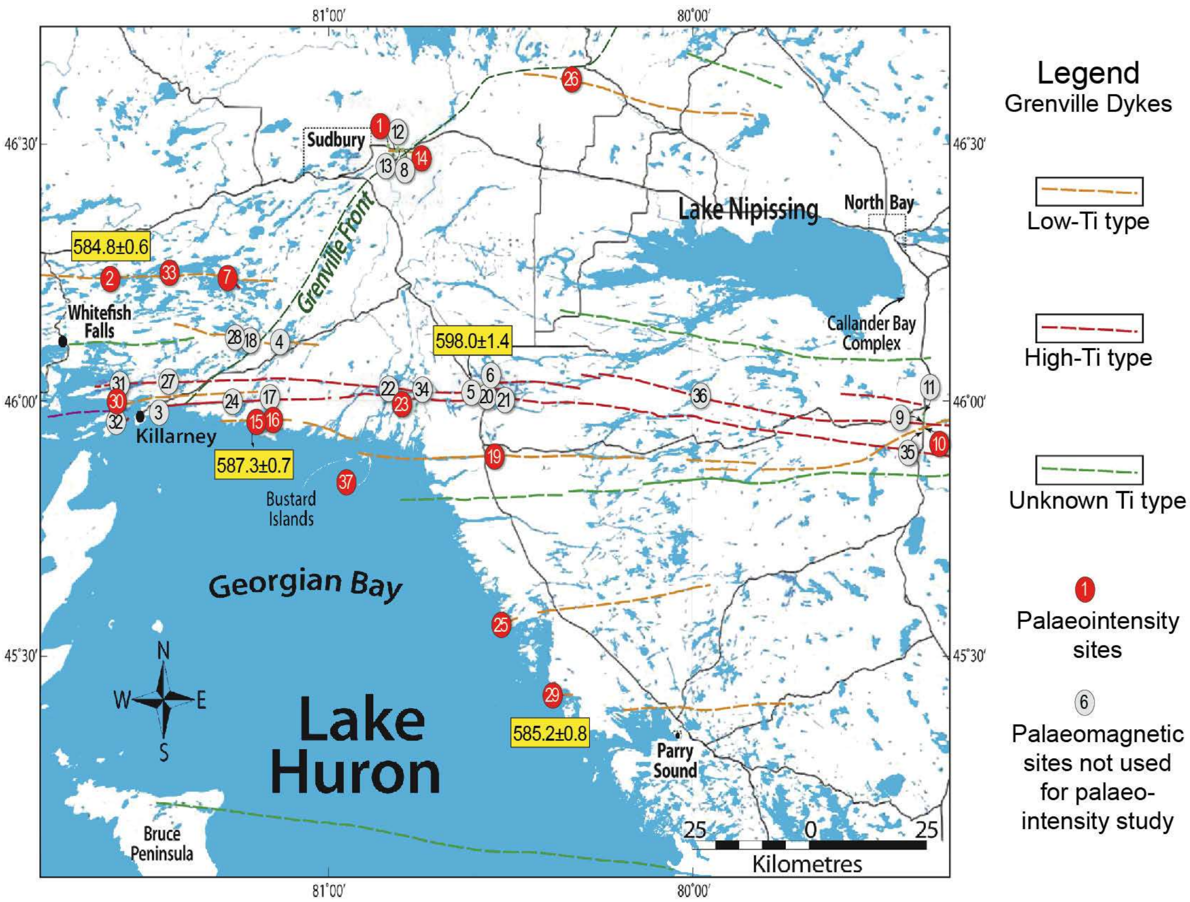

Figure 1: Map of southeast Ontario, showing the Grenville dykes and locations of sites studied in Halls et al. (2015) and sites selected for this palaeointensity study; from Halls et al. (2015)

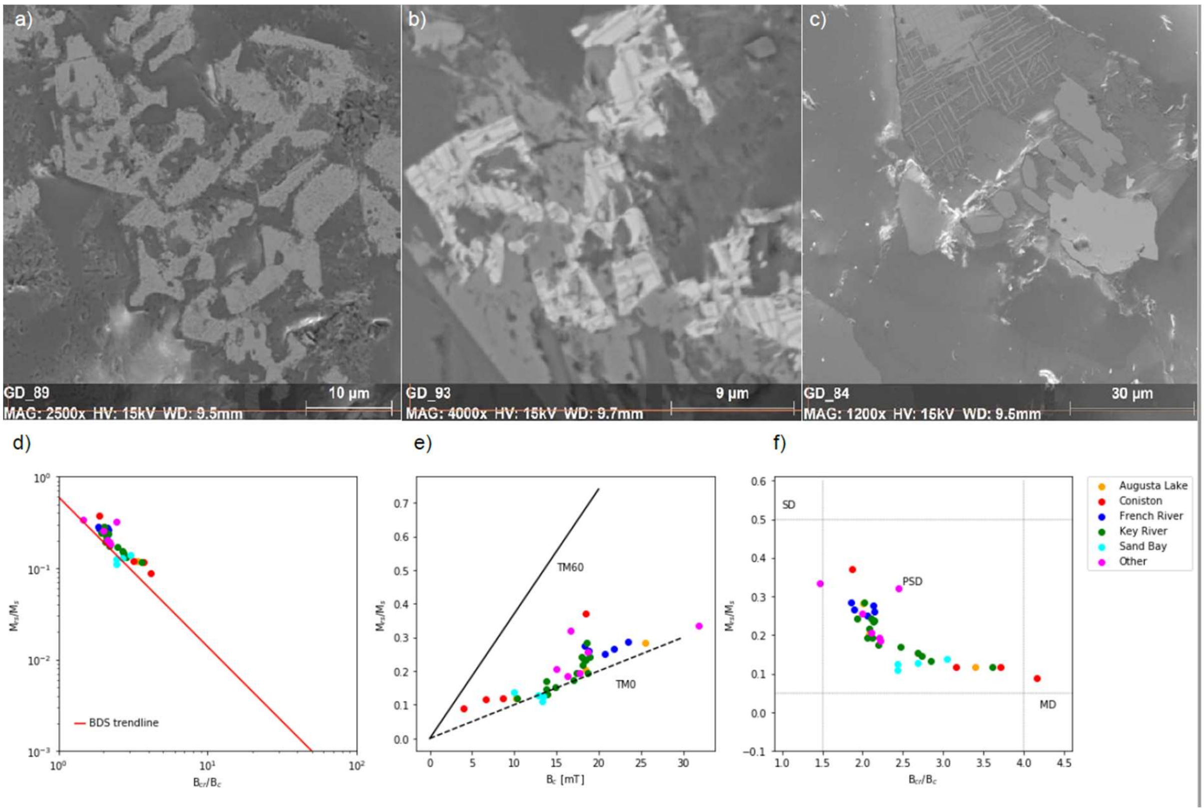

Figure 2: SEM backscatter images: (a) GD23, (b) GD29, examples of dendritic TM grains, (c) GD02, coarse Tm grain, showing magnetite-ilmenite exsolution. Plots of hysteresis parameters showing (d) Bulk Domain Stability (BDS), (e) comparison to predictions for titanomagnetites, and (f) a Day plot for representative samples of each site.

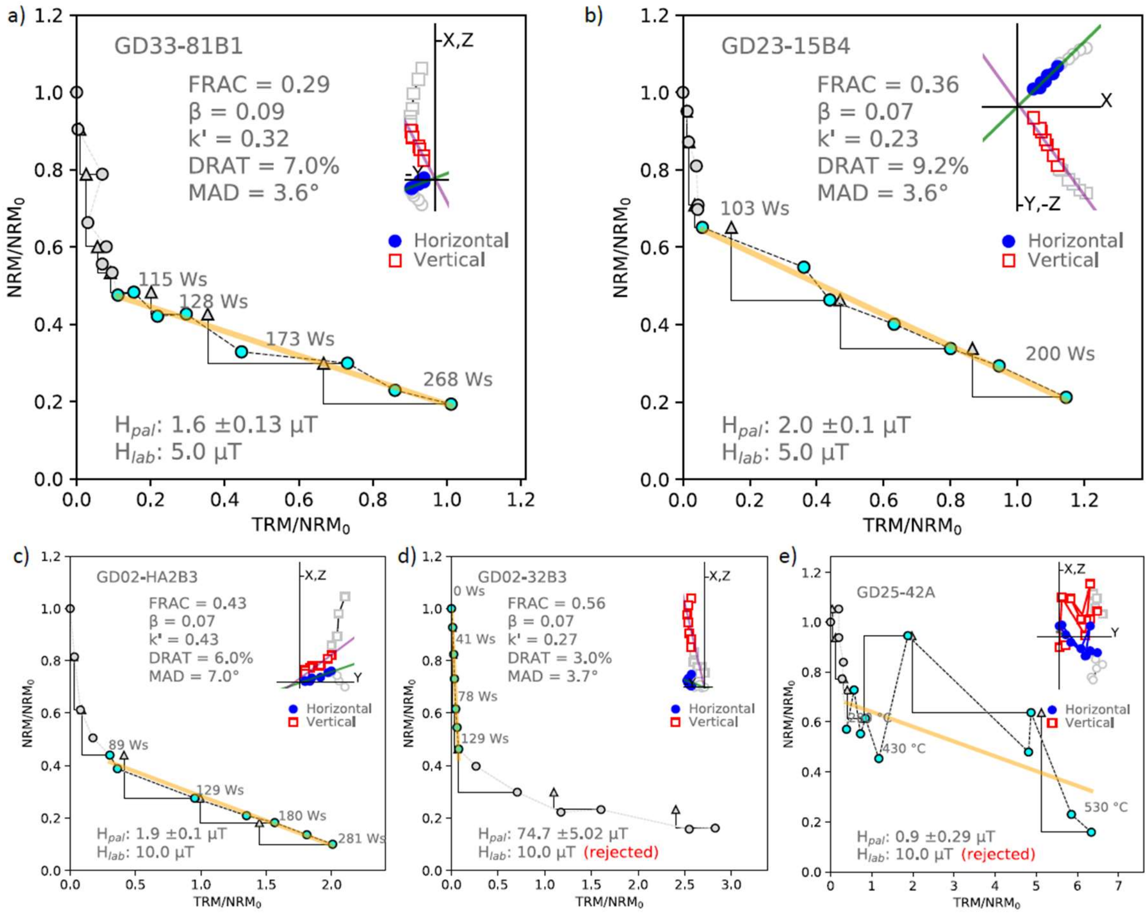

Figure 3: Arai plots of Thellier experiment results. a)-d) show microwave experiments, e) shows a result of a thermal Thellier experiment. For more details, readers are referred to section 3 of the text.

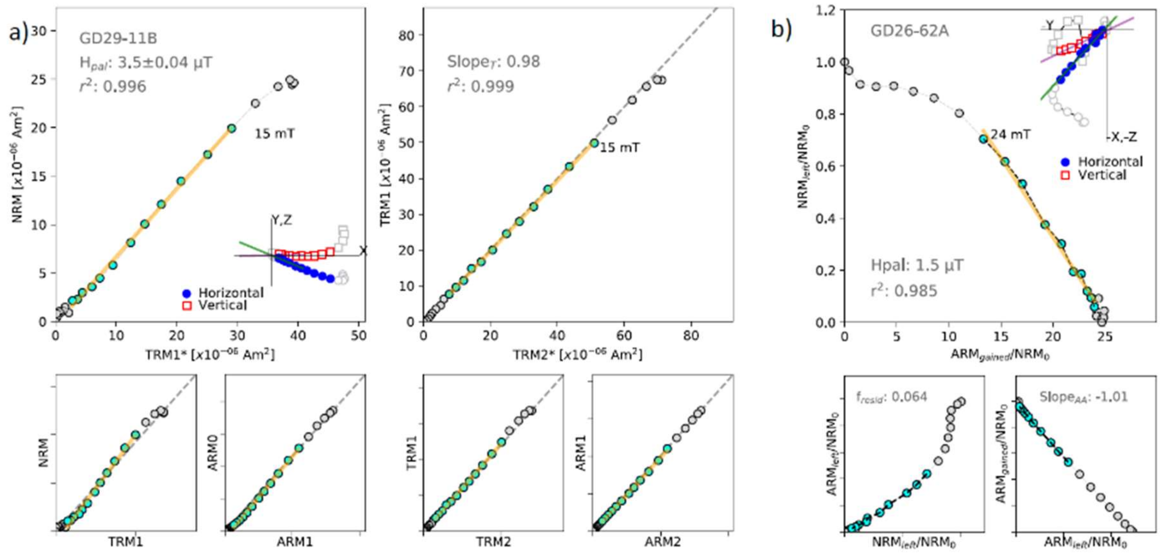

Figure 4: a) Representative example of a successful Shaw experiment: left and right columns show results from the first and second laboratory heating, respectively. The plot of NRM versus ARM corrected TRM of the first heating (TRM1*) (top left) includes the orthogonal plot of the demagnetisation of NRM; b) example of a successful pseudo-Thellier experiment: pseudo-Arai plot with orthogonal projection, demag-demag plot (NRM vs ARM) and ARM-ARM plot (acquisition vs. demagnetisation).

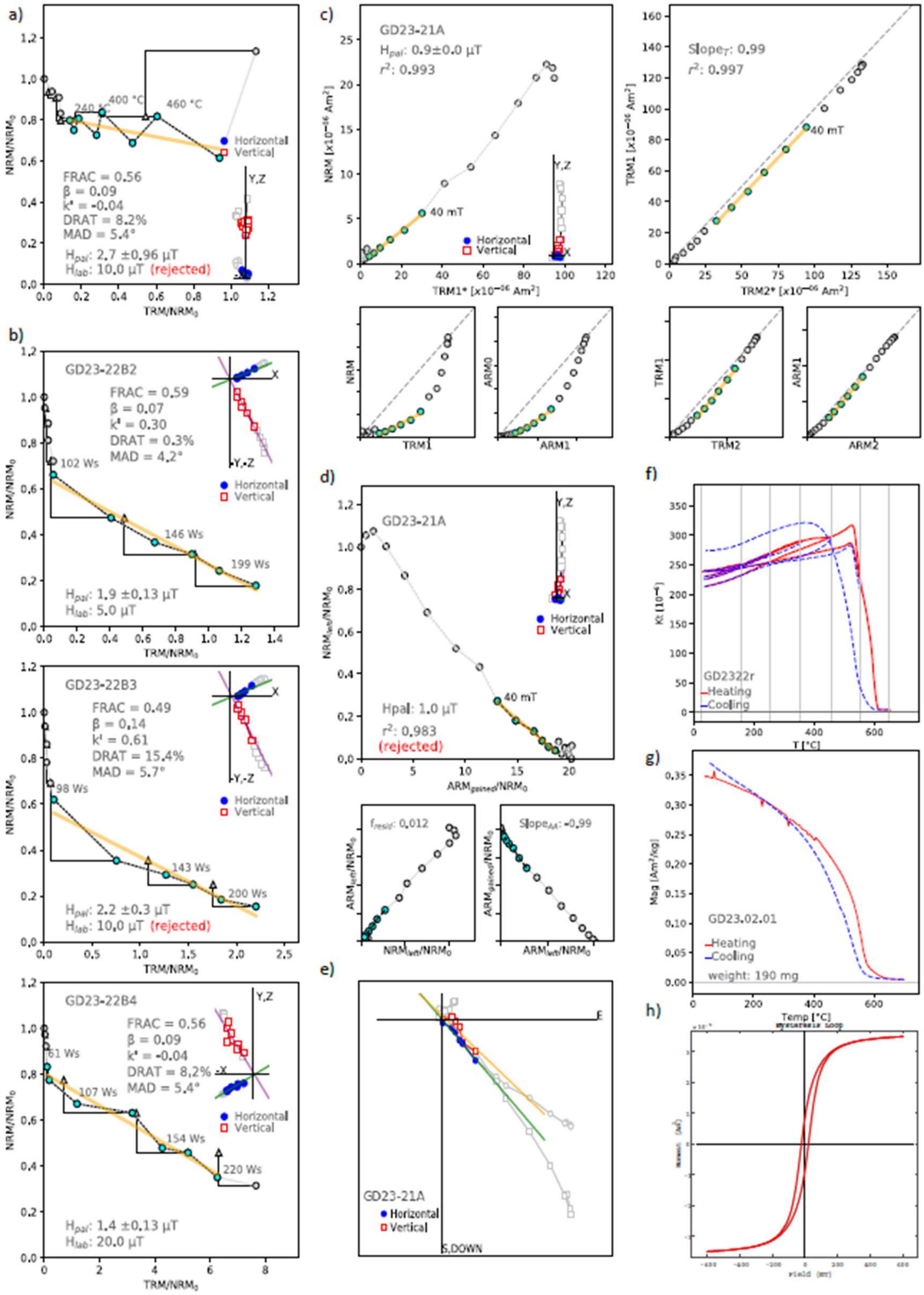

Figure 5: Compilation of results for sister specimens of sample GD23-2, all orthogonal plots for intensity experiments are shown in specimen coordinates: a) Arai plot of thermal Thellier experiment, measurement points are shown up to a temperature of 510°C; b) Arai plots of

microwave Thellier experiments; c) result of Shaw experiment; d) result of pseudo-Thellier experiment; e) Zijderveld plot in geographic coordinates; f) cyclic heatings of temperature dependent susceptibility in 100°C increments up to 650°C; g) thermomagnetic curve up to 700°C; j) temperature dependent susceptibility between 40 and 700°C; h) Hysteresis loop, analysed in HystLab (Paterson et al., 2018). Critical values of shown intensity experiments are listed in supplementary Tables 1-4.

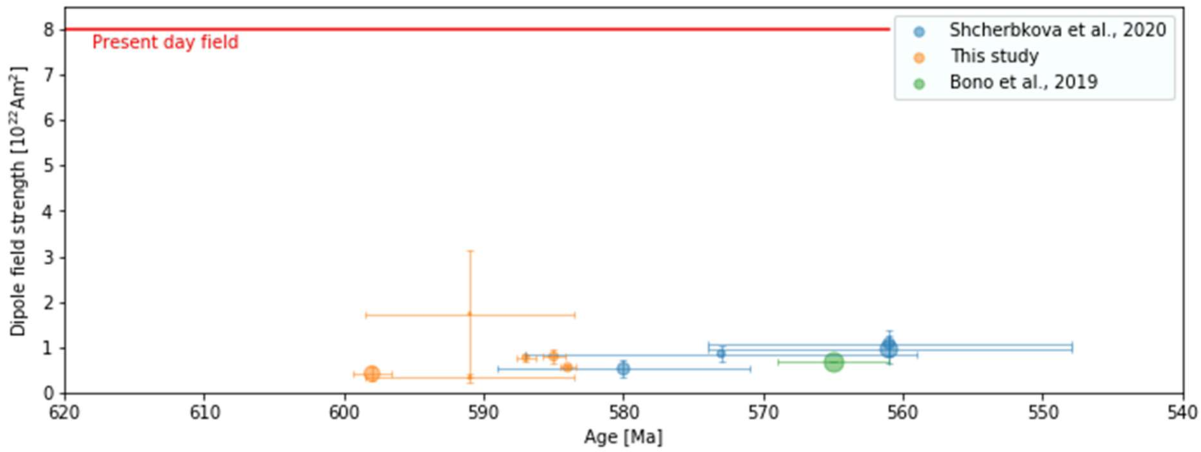

Figure 6: Virtual dipole moments of the Grenville dykes plotted versus age in with virtual dipole moments of the Baltican Volyn traps (Shcherbakova et al., 2020) and the palaeomagnetic dipole moment of the Sept Îles (Bono et al., 2019) in comparison to the present-day field strength. Marker sizes correspond to number of individual intensity estimates N used in the average. Plotted are mean values with N > 1. Error bars show estimated age errors and one standard deviation of dipole moments.

Tables:

			Directions					Intensities [μT]						pThel [μT]	VDM [$10^{22}Am^2$]		QPI
Dyke	Site	Age	N/n	Dec	Inc	a95	k	n/n_{PI}	N/n_{TH}	N/n_{MW}	N/n_S	PI	Std	PI	VDM	Std	
Augusta	GD2	584 ±0.6	10/9*	120.5	20.0	7.7	46	13/2	1/0	9/1	3/1	2.1	0.04	-	-	-	
Lake	GD33		8/6*	134	38.2	10.7	40	17/5	1/0	14/5	2/0	2.6	0.62	1.9	-	-	8
	Mean		18/15*	125.6	30.2	7.3	28	30/7	2/0	23/6	5/1	2.4	0.23	1.9	0.52	0.05	
Coniston	GD1		5/3	115.5	17.1	32.4	16	5/0	1/0	3/0	1/0	-	-	-	-	-	
	GD14		13/3	95.5	23.8	26.3	13	6/1	1/0	2/1	3/0	7.6	-	-	-	-	6
	Mean		13/3	95.5	23.8	26.3	13	11/1	2/0	5/1	4/0	7.6	-	-	1.66	x	
French River	GD23	598 ±1.4	6/3*	133.9	31.3	7.4	280	24/13	2/0	20/12	2/1	1.8	0.67	-	0.42	0.16	7
Key	GD10		10/9	137.7	-75.8	6.7	61	14/0	1/0	9/0	4/0	-	-	-	-	-	
River	GD15		5/5	140.9	-66.8	6.7	130	14/1	1/0	10/1	3/0	5.6	-	-	-	-	
	GD16		6/6*	166.7	-86.7	12.5	24	11/1	1/0	7/1	3/0	4.3	-	1.3	-	-	9
	GD19	587	9/5	100.6	-56.2	11.9	42	12/0	1/0	8/0	3/0	-	-	-	-	-	
	GD37	±0.7	9/8*	145.7	-68.2	4.2	30	7/3	1/0	2/0	4/3	5.3	1.57	3.1	-	-	
	Mean		20/19	146.2	-73.4	8.2	12	58/5	5/0	36/2	17/3	5.1	0.56	2.2	0.78	0.09	
Sand Bay	GD29	585 ±0.8	9/9*	297.7	-38.3	5.2	97	43/7	6/0	26/3	11/4	3.7	0.69	4.1	0.82	0.15	8
Other	GD07		7/6	134.8	1.2	11.2	37	3/0	0/0	0/0	3/0	-	-	-	-	-	
Grenville	GD25		9/9*	138.9	15.1	8.7	36	15/2	1/0	10/1	4/1	6.8	5.82	-	1.71	1.43	7
Dykes	GD26		9/6*	129.9	-20.2	10.8	39	8/2	1/0	4/0	3/2	1.4	0.40	1.5	0.34	0.10	6
	GD30		10/6	139	-67.3	8.4	64	5/0	1/0	3/0	1/0	-	-	-	-	-	

Table 1: Summary of palaeointensity results of the Grenville dykes: Dyke/Site: dyke/site name, Ages and directional information from Halls et al. (2015) (* directions recalculated using ChRMs from Shaw/pseudo-Thellier data, directions of sites in italics are not supported by field tests), N/n_{PI}: total number of specimens/ number of successful results, Methods: type of method that contributed successful results (MW: microwave Thellier, TH: thermal Thellier, S: Shaw), PI: palaeointensity results in μT, Std: standard deviation of palaeointensity results , pThel: palaeointensity results in μT from pseudo-Thellier experiments. Values are shown as comparison to the results from the heating methods but are not used in the calculation of the mean palaeointensities. VDM: virtual dipole moment in $10^{22}Am^2$, Std: standard deviation of VDM results, QPI values of sites.

References:

Abrajevitch, A., Van der Voo, R., 2010. Incompatible Ediacaran paleomagnetic directions suggest an equatorial geomagnetic dipole hypothesis. Earth Planet. Sci. Lett. 293, 164–170. https://doi.org/10.1016/j.epsl.2010.02.038

Aubert, J., Wicht, J., 2004. Axial vs. equatorial dipolar dynamo models with implications for planetary magnetic fields. Earth Planet. Sci. Lett. 221, 409–419. https://doi.org/10.1016/S0012-821X(04)00102-5

Bazhenov, M.L., Levashova, N.M., Meert, J.G., Golovanova, I. V., Danukalov, K.N., Fedorova, N.M., 2016. Late Ediacaran magnetostratigraphy of Baltica: Evidence for Magnetic Field Hyperactivity? Earth Planet. Sci. Lett. 435, 124–135. https://doi.org/10.1016/j.epsl.2015.12.015

Béguin, A., Paterson, G.A., Biggin, A.J., de Groot, L. V., 2020. Paleointensity.org: An Online, Open Source, Application for the Interpretation of Paleointensity Data. Geochemistry, Geophys. Geosystems 21, 1–15. https://doi.org/10.1029/2019GC008791

Biggin, A.J., 2010. Are systematic differences between thermal and microwave Thellier-type palaeointensity estimates a consequence of multidomain bias in the thermal results? Phys. Earth Planet. Inter. 180, 16–40. https://doi.org/10.1016/j.pepi.2010.03.005

Biggin, A.J., Paterson, G.A., 2014. A new set of qualitative reliability criteria to aid inferences on palaeomagnetic dipole moment variations through geological time. Front. Earth Sci. 2, 1–9. https://doi.org/10.3389/feart.2014.00024

Biggin, A.J., Perrin, M., Dekkers, M.J., 2007a. A reliable absolute palaeointensity determination obtained from a non-ideal recorder. Earth Planet. Sci. Lett. 257, 545–

563. https://doi.org/10.1016/j.epsl.2007.03.017

Biggin, A.J., Perrin, M., Shaw, J., 2007b. A comparison of a quasi-perpendicular method of absolute palaeointensity determination with other thermal and microwave techniques. Earth Planet. Sci. Lett. 257, 564–581. https://doi.org/10.1016/j.epsl.2007.03.016

Biggin, A.J., Piispa, E.J., Pesonen, L.J., Holme, R., Paterson, G.A., Veikkolainen, T., Tauxe, L., 2015. Palaeomagnetic field intensity variations suggest Mesoproterozoic inner-core nucleation. Nature 526, 245–248. https://doi.org/10.1038/nature15523

Bono, R.K., Tarduno, J.A., 2015. A stable ediacaran earth recorded by single silicate crystals of the ca. 565 Ma sept-Îles intrusion. Geology 43, 131–134. https://doi.org/10.1130/G36247.1

Bono, R.K., Tarduno, J.A., Nimmo, F., Cottrell, R.D., 2019. Young inner core inferred from Ediacaran ultra-low geomagnetic field intensity. Nat. Geosci. 12, 143–147. https://doi.org/10.1038/s41561-018-0288-0

Brown, M.C., Gratton, M.N., Shaw, J., Holme, R., Soler, V., 2009. Microwave palaeointensity results from the Matuyama-Brunhes geomagnetic field reversal. Phys. Earth Planet. Inter. 173, 75–102. https://doi.org/10.1016/j.pepi.2008.11.001

Day, R., Fuller, M., Schmidt, V.A., 1977. Hysteresis properties of titanomagnetites: Grain-size and compositional dependence. Phys. Earth Planet. Inter. 13, 260–267. https://doi.org/10.1016/0031-9201(77)90108-X

De Groot, L. V., Biggin, A.J., Dekkers, M.J., Langereis, C.G., Herrero-Bervera, E., 2013. Rapid regional perturbations to the recent global geomagnetic decay revealed by a new Hawaiian record. Nat. Commun. 4, 1–7. https://doi.org/10.1038/ncomms3727

Doubrovine, P. V., Veikkolainen, T., Pesonen, L.J., Piispa, E., Ots, S., Smirnov, A. V., Kulakov, E. V., Biggin, A.J., 2019. Latitude Dependence of Geomagnetic Paleosecular Variation and its Relation to the Frequency of Magnetic Reversals: Observations From the Cretaceous and Jurassic. Geochemistry, Geophys. Geosystems 20, 1240–1279. https://doi.org/10.1029/2018GC007863

Driscoll, P.E., Evans, D.A.D., 2016. Frequency of Proterozoic geomagnetic superchrons. Earth Planet. Sci. Lett. 437, 9–14. https://doi.org/10.1016/j.epsl.2015.12.035

Evans, D.A.D., Raub, T.D., 2011. Chapter 7: Neoproterozoic glacial palaeolatitudes: A global update, in: Geological Society Memoir. pp. 93–112. https://doi.org/10.1144/M36.7

Gissinger, C., Petitdemange, L., Schrinner, M., Dormy, E., 2012. Bistability between equatorial and axial dipoles during magnetic field reversals. Phys. Rev. Lett. 108. https://doi.org/10.1103/PhysRevLett.108.234501

Grappone, J.M., Biggin, A.J., Barrett, T.J., Hill, M.J., Sprain, C.J., 2020. Comparison of Thermal and Microwave Paleointensity Estimates in Specimens Displaying Non-Ideal Behavior in Thellier-Style Paleointensity Experiments. J. Geophys. Res. Solid Earth 125. https://doi.org/10.1029/2020JB019802

Grappone, J.M., Biggin, A.J., Hill, M.J., 2019. Solving the mystery of the 1960 Hawaiian lava flow: Implications for estimating Earth's magnetic field. Geophys. J. Int. 218, 1796–1806. https://doi.org/10.1093/gji/ggz252

Halls, H.C., Lovette, A., Hamilton, M., Söderlund, U., 2015. A paleomagnetic and U-Pb geochronology study of the western end of the Grenville dyke swarm: Rapid changes in paleomagnetic field direction at ca. 585Ma related to polarity reversals? Precambrian

Res. 257, 137–166. https://doi.org/10.1016/j.precamres.2014.11.029

Halls, H.C., McArdle, N.J., Gratton, M.N., Hill, M.J., Shaw, J., 2004. Microwave paleointensities from dyke chilled margins: A way to obtain long-term variations in geodynamo intensity for the last three billion years. Phys. Earth Planet. Inter. 147, 183–195. https://doi.org/10.1016/j.pepi.2004.03.013

Hawkins, L.M.A., Anwar, T., Shcherbakova, V. V., Biggin, A.J., Kravchinsky, V.A., Shatsillo, A. V., Pavlov, V.E., 2019. An exceptionally weak Devonian geomagnetic field recorded by the Viluy Traps, Siberia. Earth Planet. Sci. Lett. 506, 134–145. https://doi.org/10.1016/j.epsl.2018.10.035

Hodych, J.P., Cox, R.A., Košler, J., 2004. An equatorial Laurentia at 550 Ma confirmed by Grenvillian inherited zircons dated by LAM ICP-MS in the Skinner Cove volcanics of western Newfoundland: Implications for inertial interchange true polar wander. Precambrian Res. 129, 93–113. https://doi.org/10.1016/j.precamres.2003.10.012

Hyodo, H., Dunlop, D.J., 1993. Effect of anisotropy on the paleomagnetic contact test for a Grenville Dike. J. Geophys. Res. 98, 7997–8017. https://doi.org/10.1029/92JB02915

Johnson, C.L., Mittelholz, A., Langlais, B., Russell, C.T., Ansan, V., Banfield, D., Chi, P.J., Fillingim, M.O., Forget, F., Haviland, H.F., Golombek, M., Joy, S., Lognonné, P., Liu, X., Michaut, C., Pan, L., Quantin-Nataf, C., Spiga, A., Stanley, S., Thorne, S.N., Wieczorek, M.A., Yu, Y., Smrekar, S.E., Banerdt, W.B., 2020. Crustal and time-varying magnetic fields at the InSight landing site on Mars. Nat. Geosci. 13, 199–204. https://doi.org/10.1038/s41561-020-0537-x

Kirschvink, J.L., Ripperdan, R.L., Evans, D.A., 1997. Evidence for a large-scale reorganization of Early Cambrian continental masses by inertial interchange true polar wander. Science (80-.). 277, 541–545. https://doi.org/10.1126/science.277.5325.541

Kissel, C., Laj, C., 2004. Improvements in procedure and paleointensity selection criteria (PICRIT-03) for Thellier and Thellier determinations: Application to Hawaiian basaltic long cores. Phys. Earth Planet. Inter. 147, 155–169. https://doi.org/10.1016/j.pepi.2004.06.010

Kulakov, E. V., Sprain, C.J., Doubrovine, P. V., Smirnov, A. V., Paterson, G.A., Hawkins, L., Fairchild, L., Piispa, E.J., Biggin, A.J., 2019. Analysis of an Updated Paleointensity Database (QPI-PINT) for 65–200 Ma: Implications for the Long-Term History of Dipole Moment Through the Mesozoic. J. Geophys. Res. Solid Earth 124, 9999–10022. https://doi.org/10.1029/2018JB017287

Lawley, E.A., 1970. The intensity of the geomagnetic field in Iceland during neogene polarity transitions and systematic deviations. Earth Planet. Sci. Lett. 10, 145–149. https://doi.org/10.1016/0012-821X(70)90076-2

Leonhardt, R., Soffel, H.C., 2002. A reversal of the Earth’s magnetic field recorded in mid-Miocene lava flows of Gran Canaria: Paleointensities. J. Geophys. Res. Solid Earth 107, EPM 5-1-EPM 5-11. https://doi.org/10.1029/2001jb000949

Levashova, N.M., Golovanova, I. V., Rudko, D. V., Danukalov, K.N., Rudko, S. V., Yu, S.R., Meert, J.G., 2021. Late Ediacaran magnetic field hyperactivity: Quantifying the reversal frequency in the Zigan Formation, Southern Urals, Russia. Gondwana Res. 94, 133–142. https://doi.org/10.1016/j.gr.2021.02.018

Li, Z.X., Evans, D.A.D., Halverson, G.P., 2013. Neoproterozoic glaciations in a revised global palaeogeography from the breakup of Rodinia to the assembly of Gondwanaland. Sediment. Geol. 294, 219–232. https://doi.org/10.1016/j.sedgeo.2013.05.016

McCausland, P.J.A., Hodych, J.P., 1998. Paleomagnetism of the 550 Ma Skinner Cove volcanics of western Newfoundland and the opening of the Iapetus Ocean. Earth Planet. Sci. Lett. 163, 15–29. https://doi.org/10.1016/S0012-821X(98)00171-X

McCausland, P.J.A., Van der Voo, R., Hall, C.M., 2007. Circum-Iapetus paleogeography of the Precambrian-Cambrian transition with a new paleomagnetic constraint from Laurentia. Precambrian Res. 156, 125–152. https://doi.org/10.1016/j.precamres.2007.03.004

Meert, J.G., 2014. Ediacaran-Early Ordovician paleomagnetism of Baltica: A review. Gondwana Res. 25, 159–169. https://doi.org/10.1016/j.gr.2013.02.003

Paterson, G.A., 2011. A simple test for the presence of multidomain behavior during paleointensity experiments. J. Geophys. Res. Solid Earth 116. https://doi.org/10.1029/2011JB008369

Paterson, G.A., Heslop, D., Muxworthy, A.R., 2010. Deriving confidence in paleointensity estimates. Geochemistry, Geophys. Geosystems 11. https://doi.org/10.1029/2010GC003071

Paterson, G.A., Heslop, D., Pan, Y., 2016. The pseudo-Thellier palaeointensity method: New calibration and uncertainty estimates. Geophys. J. Int. 207, 1596–1608. https://doi.org/10.1093/gji/ggw349

Paterson, G.A., Muxworthy, A.R., Yamamoto, Y., Pan, Y., 2017. Bulk magnetic domain stability controls paleointensity fidelity. Proc. Natl. Acad. Sci. U. S. A. 114, 13120–13125. https://doi.org/10.1073/pnas.1714047114

Paterson, G.A., Tauxe, L., Biggin, A.J., Shaar, R., Jonestrask, L.C., 2014. On improving the selection of Thellier-type paleointensity data. Geochemistry, Geophys. Geosystems 15, 1180–1192. https://doi.org/10.1002/2013GC005135

Paterson, G.A., Zhao, X., Jackson, M., Heslop, D., 2018. Measuring, Processing, and Analyzing Hysteresis Data. Geochemistry, Geophys. Geosystems 19, 1925–1945. https://doi.org/10.1029/2018GC007620

Prévot, M., 1981. Some aspects of magnetic viscosity in subaerial and submarine volcanic rocks. Geophys. J. R. Astron. Soc. 66, 169–192. https://doi.org/10.1111/j.1365-246X.1981.tb05952.x

Prevot, M., Mankinen, E.A., Coe, R.S., Gromme, C.S., 1985. The Steens Mountain (Oregon) geomagnetic polarity transition 2. Field intensity variations and discussion of reversal models (USA) . J. Geophys. Res. 90. https://doi.org/10.1029/jb090ib12p10417

Riisager, P., Riisager, J., 2001. Detecting multidomain magnetic grains in Thellier palaeointensity experiments. Phys. Earth Planet. Inter. 125, 111–117. https://doi.org/10.1016/S0031-9201(01)00236-9

Robert, B., Besse, J., Blein, O., Greff-Lefftz, M., Baudin, T., Lopes, F., Meslouh, S., Belbadaoui, M., 2017. Constraints on the Ediacaran inertial interchange true polar wander hypothesis: A new paleomagnetic study in Morocco (West African Craton). Precambrian Res. 295, 90–116. https://doi.org/10.1016/j.precamres.2017.04.010

Rolph, T.C., Shaw, J., 1985. A new method of palaeofield magnitude correction for thermally altered samples and its application to Lower Carboniferous lavas. Geophys. J. R. Astron. Soc. 80, 773–781. https://doi.org/10.1111/j.1365-246X.1985.tb05124.x

Schmidt, P.W., Williams, G.E., 2010. Ediacaran palaeomagnetism and apparent polar wander path for Australia: No large true polar wander. Geophys. J. Int. 182, 711–726. https://doi.org/10.1111/j.1365-246X.2010.04652.x

Shaar, R., Tauxe, L., 2015. Instability of thermoremanence and the problem of estimating the ancient geomagnetic field strength from non-single-domain recorders. Proc. Natl. Acad. Sci. U. S. A. 112, 11187–11192. https://doi.org/10.1073/pnas.1507986112

Shcherbakov, V.P., Gribov, S.K., Lhuillier, F., Aphinogenova, N.A., Tsel'movich, V.A., 2019. On the Reliability of Absolute Palaeointensity Determinations on basaltic Rocks Bearing a Thermochemical Remanence. J. Geophys. Res. Solid Earth 124, 7616–7632. https://doi.org/10.1029/2019JB017873

Shcherbakova, V. V., Bakhmutov, V.G., Thallner, D., Shcherbakov, V.P., Zhidkov, G. V., Biggin, A.J., 2020. Ultra-low palaeointensities from East European Craton, Ukraine support a globally anomalous palaeomagnetic field in the Ediacaran. Geophys. J. Int. 220, 1920–1946. https://doi.org/10.1093/gji/ggz566

Shcherbakova, V. V., Biggin, A.J., Veselovskiy, R. V., Shatsillo, A. V., Hawkins, L.M.A., Shcherbakov, V.P., Zhidkov, G. V., 2017. Was the Devonian geomagnetic field dipolar or multipolar? Palaeointensity studies of Devonian igneous rocks from the Minusa Basin (Siberia) and the Kola Peninsula dykes, Russia. Geophys. J. Int. 209, 1265–1286. https://doi.org/10.1093/gji/ggx085

Smirnov, A. V., Kulakov, E. V., Foucher, M.S., Bristol, K.E., 2017. Intrinsic paleointensity bias and the long-term history of the geodynamo. Sci. Adv. 3. https://doi.org/10.1126/sciadv.1602306

Smirnov, A. V., Tarduno, J.A., 2005. Thermochemical remanent magnetization in Precambrian rocks: Are we sure the geomagnetic field was weak? J. Geophys. Res. Solid Earth 110, 1–12. https://doi.org/10.1029/2004JB003445

Suttie, N., Shaw, J., Hill, M.J., 2010. Direct demonstration of microwave demagnetization of a whole rock sample with minimal heating. Earth Planet. Sci. Lett. 292, 357–362. https://doi.org/10.1016/j.epsl.2010.02.002

Tanaka, H., Komuro, N., 2009. The Shaw paleointensity method: Can the ARM simulate the TRM alteration? Phys. Earth Planet. Inter. 173, 269–278. https://doi.org/10.1016/j.pepi.2009.01.003

Tarduno, J.A., Cottrell, R.D., 2005. Dipole strength and variation of the time-averaged reversing and nonreversing geodynamo based on Thellier analyses of single plagioclase crystals. J. Geophys. Res. Solid Earth 110, 1–10. https://doi.org/10.1029/2005JB003970

Tauxe, L., Gee, J.S., Steiner, M.B., Staudigel, H., 2013. Paleointensity results from the Jurassic: New constraints from submarine basaltic glasses of ODP Site 801C. Geochemistry, Geophys. Geosystems 14, 4718–4733. https://doi.org/10.1002/ggge.20282

Tauxe, L., Staudigel, H., 2004. Strength of the geomagnetic field in the cretaceous normal superchron: New data from submarine basaltic glass of the troodos ophiolite. Geochemistry, Geophys. Geosystems 5. https://doi.org/10.1029/2003GC000635

Thellier, E., 1941. Sur la vérification d’une méthode permettant de déterminer l’intensité du champ terrestre dans le passé. Comptes rendus l’Académie des Sci. 212, 281–283.

Torsvik, T.H., 1998. Polar Wander and the Cambrian. Science (80-.). 279, 9a – 9.

https://doi.org/10.1126/science.279.5347.9a

Tsai, V.C., Stevenson, D.J., 2007. Theoretical constraints on true polar wander. J. Geophys. Res. Solid Earth 112. https://doi.org/10.1029/2005JB003923

Tsunakawa, H., Shaw, J., 1994. The Shaw method of palaeointensity determinations and its application to recent volcanic rocks. Geophys. J. Int. 118, 781–787. https://doi.org/10.1111/j.1365-246X.1994.tb03999.x

Ueno, H., Irving, E., McNutt, R.H., 1975. Paleomagnetism of the Whitestone Anorthosite and Diorite, the Grenville Polar Track, and Relative Motions of the Laurentian and Baltic Shields. Can. J. Earth Sci. 12, 209–226. https://doi.org/10.1139/e75-019

Ueno, N., 1995. Geomagnetic Paleointensity Experiment on Igneous and Metamorphic Rocks From Enderby Land in Napier Complex, Antarctica. Proc. NIPR Symp. Antarct. Geosci. 8, 193–200.

Veikkolainen, T., Pesonen, L.J., 2014. Palaeosecular variation, field reversals and the stability of the geodynamo in the Precambrian. Geophys. J. Int. 199, 1515–1526. https://doi.org/10.1093/gji/ggu348

Wang, D., Van der Voo, R., 2004. The hysteresis properties of multidomain magnetite and titanomagnetite/titanomaghemite in mid-ocean ridge basalts. Earth Planet. Sci. Lett. 220, 175–184. https://doi.org/10.1016/S0012-821X(04)00052-4

Xiao, S.H., Narbonne, G.M., 2020. The Ediacaran Period, in: Geologic Time Scale 2020. BV, pp. 521–561. https://doi.org/10.1016/b978-0-12-824360-2.00018-8

Yamamoto, Y., Shibuya, H., Tanaka, H., Hoshizumi, H., 2010. Geomagnetic paleointensity deduced for the last 300kyr from Unzen Volcano, Japan, and the dipolar nature of the

Iceland Basin excursion. Earth Planet. Sci. Lett. 293, 236–249. https://doi.org/10.1016/j.epsl.2010.02.024

Yoshihara, A., Hamano, Y., 2004. Paleomagnetic constraints on the Archean geomagnetic field intensity obtained from komatiites of the Barberton and Belingwe greenstone belts, South Africa and Zimbabwe. Precambrian Res. 131, 111–142. https://doi.org/10.1016/j.precamres.2004.01.003

Yu, Y., Tauxe, L., 2005. Testing the IZZI protocol of geomagnetic field intensity determination. Geochemistry, Geophys. Geosystems 6. https://doi.org/10.1029/2004GC000840